Putting Neutron Scattering into Perspective

H. Schober
Institut Laue-Langevin, F-38042 Grenoble, France

August 31, 2003

1 Introduction

Whenever it is important to know precisely where atoms are or how atoms move one should consider a neutron scattering investigation. Neutron scattering is a very powerful probe of microscopic structure and dynamics. In order to use it to its best a number of facts have to be known. The strength of neutron scattering resides in its simplicity. Although neutron scattering is often termed a heavy experimental technique due to the fact that it requires complex and, therefore, expensive equipment, it is actually very difficult to conceive a simpler scattering event than that of thermal or cold neutrons. *Why is that so?* Due to the short range of the weak interaction – a few fm – with respect to the wavelength of the neutron – a few Å– the scattering is isotropic, i.e. only s-waves are required in the expansion of the scattered wavefunction [3]. Due to this isotropy the scattering can be described by a scalar which is the scattering amplitude b. The complex part of b takes care of absorption. As the scattering is generally weak the incoming neutron flux can be considered constant and multiple scattering events as rare for reasonable scattering volumes.[1] This implies that we can work in the lowest order of perturbation i.e. in the Born approximation.
In this article we will develop the above outlined arguments and introduce the main concepts that are necessary to understand how physically meaningful information can be extracted from the raw experimental data.

[1] In all experiments we should as a rule of thumb try to work with sample volumes such that at most 10% of the neutrons are scattered while 90 % are travelling unperturbed into the forward direction. This "waste' of neutrons is required to obtain clean and easy to interpret results.

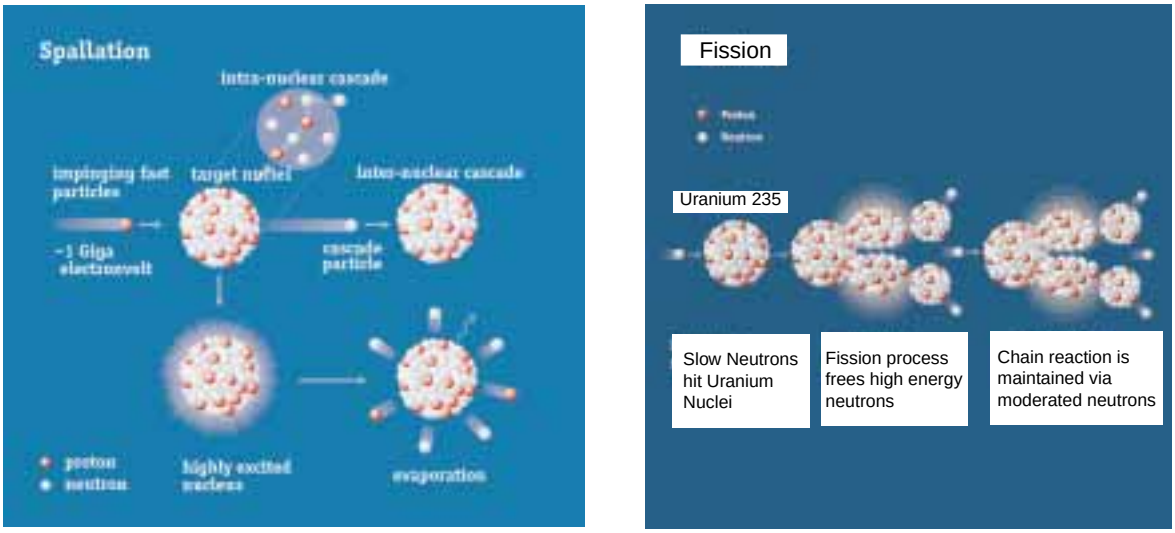

Figure 1: Schematics of spallation and fission processes

2 Neutron Sources

2.1 Method of production

Free neutrons are produced via the excitation of nuclei. In the case of fission slow neutrons interact with metastable ^{235}U nuclei. The excited nucleus decays in a cascade of fission products. In the average 2.5 neutrons are produced by the fission of one ^{235}U nucleus. These neutrons possess very elevated energies of about 2 MeV and are thus unsuitable for inducing further fission processes. With the help of moderators the fast neutrons are slowed down to meV energies. These slow neutrons sustain the chain reaction in a nuclear reactor. By allowing some of the moderated neutrons to escape from the core region free neutrons for scientific use are obtained.
In the case of spallation high energy protons produced by an accelerator hit metallic targets like uranium, tungsten lead or mercury. The thus excited nuclei boil of particles. Among those we encounter up to 20 neutrons. Like in the case of fission these high energy neutrons have to be moderated.

2.2 Characteristics of the source

In a standard reactor neutrons are produced at a constant rate. The flux of neutrons thus has no explicit time structure. We are dealing with a continuous neutron source. Typical examples of continuous neutron sources are the ILL reactor in Grenoble (see figure 2), France or the new Munich reactor in Germany. Quasi-continuous neutron beams can equally be obtained via spallation. This is the case at the PSI in Villigen, Switzerland.
In many cases it can be advantageous to work with pulsed neutron beams as this

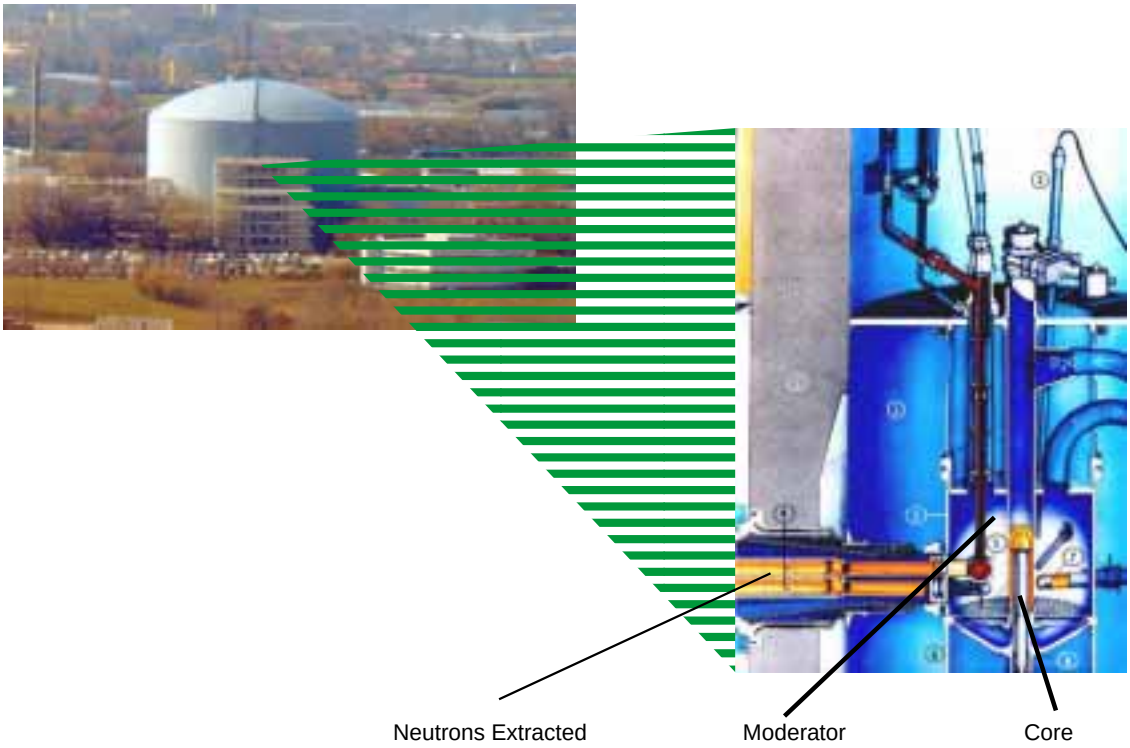

Figure 2: The worlds most powerful continuous neutron source is the ILL reactor in Grenoble, France. High energy neutrons are produced via nuclear fission of ^{235}U in the core of the reactor. They are moderated in the surrounding D_2O leading to a Maxwell energy distribution centered at about 25 meV. Apart from these thermal neutrons, cold and hot neutrons re obtained via appropriate hot and cold moderators. The high flux is achieved by a compact core design in combination with high thermal power (57 MW).

allows to determine the neutron energies by simply measuring the time of flight. At a continuous neutron source this is achieved by mechanical chopping devices incorporated into the spectrometer design. The production of pulsed neutron beams directly at the source is rather simple in the case of spallation. It is sufficient to bunch the protons in the accelerator. Depending on the time structure of the proton beam and the characteristics of the moderator neutron pulses as short as a few microseconds can be produced at adapted rates of 50 or 60 Hz. This principle is used at the pulsed spallation sources like ISIS (see figure 3) in the UK the SNS in the US or J-SNS in Japan.
What is important for the following discussion is the *incoherent nature* of these neutron sources. Both the production and moderation is accomplished via completely random events. Neutron sources thus have to be compared to light bulbs in optics. The lack of coherence, if translated into quantum mechanics, implies that there is no correlation of the phases of the neutron wave fields emanating from different regions of the source. As the moderation of the neutrons is done via collisions in a thermal bath (for example constituted of D_2O, H_2 or D_2 molecules in the liquid state) the spectrum of the moder-

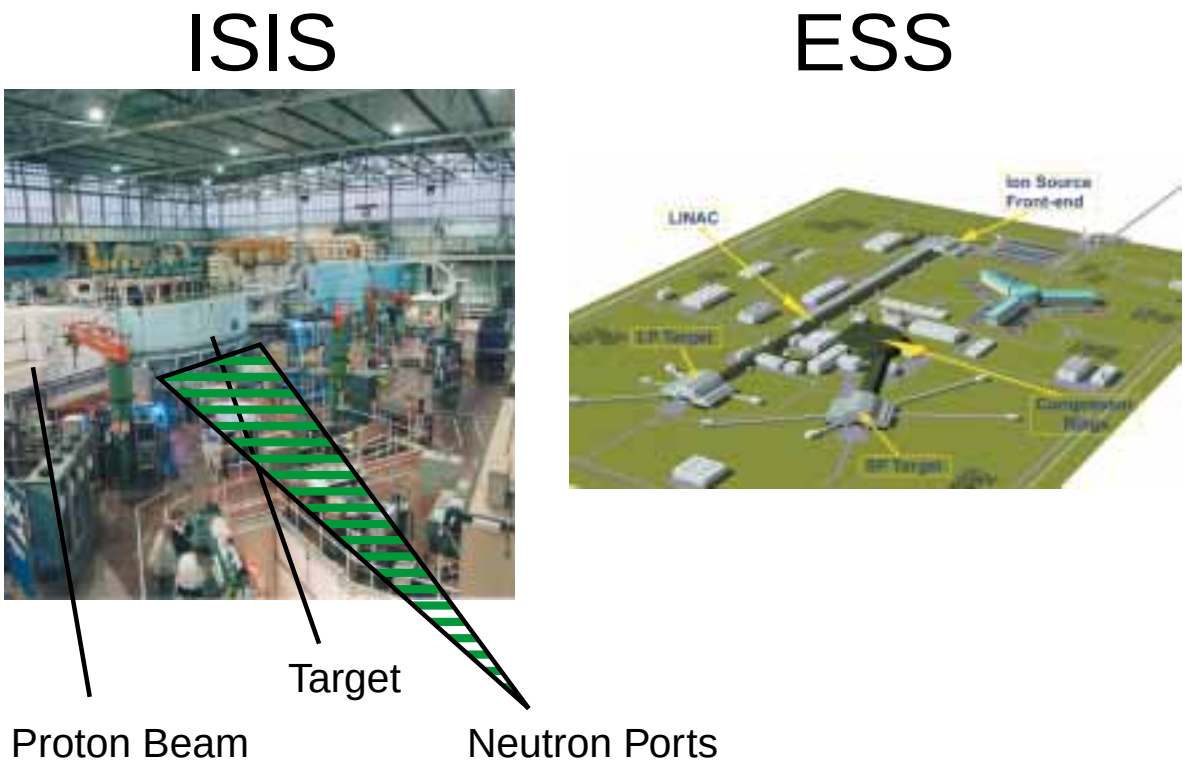

Figure 3: The worlds most powerful pulsed neutron source is currently ISIS in the UK. So-called MW spallation sources are currently under construction in the US and Japan. The European ESS project combined a short with a long pulse spallation source. Bunches of protons hit the target of the spallation source creating bursts of high energy neutrons. Like in a reactor these are moderated to thermal or cold energies.

ated neutrons follows a Maxwell-Boltzmann distribution governed by the temperature oof the bath:

$$\Phi(E)dE = \Phi_{\text{thermal}} \frac{2}{\pi} \frac{\sqrt{E}}{(k_b T)^{3/2}} \exp\left(-\frac{E}{k_b T}\right) dE. \tag{1}$$

The colder the moderator the lower is the mean energy of the neutrons (see figure 4). Apart from this the beam equally contains fast and epithermal neutrons that escaped to moderator before they become fully thermalized.
A generally accepted classification is given as

1. epithermal above 500 meV
2. hot from 100 to 500 meV
3. thermal from 10 to 100 meV
4. cold below 10 meV

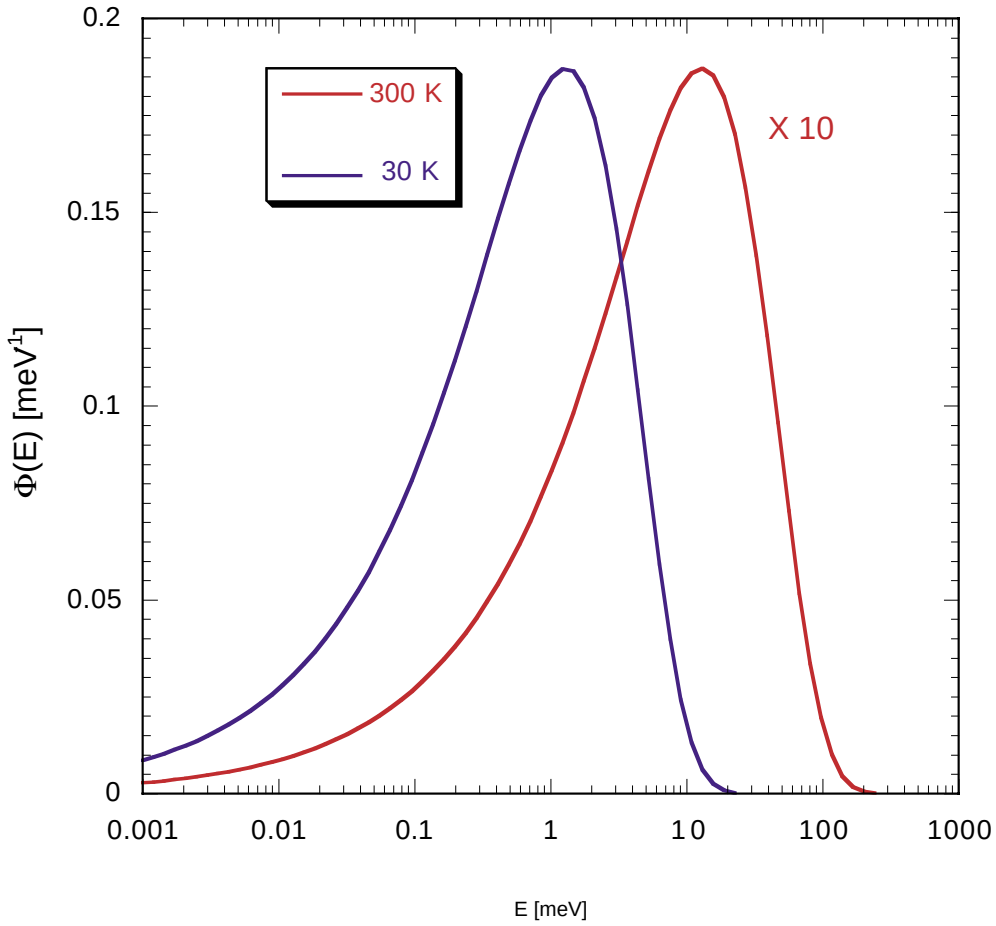

Figure 4: Maxwell Boltzmann distribution for moderator energies of 300 K and 30 K, respectively. The y-scale has to be scaled by the interated flux ϕ_{thermal} which is assumed here to be 10 times higher at 300 K.

3 The scattering of slow neutrons by condensed matter

3.1 Basic properties of slow neutrons

Neutrons are chargeless massive particles carrying a spin of $\frac{1}{2}$. They interact with nuclear matter via the strong interaction. Due to the magnetic moment associated with their spin they equally react to the presence of magnetic fields. The nuclear and magnetic interactions are similar in strength. For this reason neutrons are the ideal probe for studying magnetic structure and dynamics. As neutrons carry no electric charge they experience no Coulomb barrier and thus penetrate deeply into matter unless confronted with absorbing nuclei like Li, Cd or Gd.

The energy of a free neutron is related to its classical speed via

$$E = \frac{1}{2}mv^2 = \frac{\hbar^2 k^2}{2m}, \qquad k = \frac{2\pi}{\lambda}. \tag{2}$$

$\vec{k}$ is the wavevector of the matter wave associated with the free neutron of well-defined linear momentum $\vec{p} = \hbar\vec{k}$.
Using standard units we get the useful relation

$$E[\text{meV}] = 81.796 \cdot \lambda^{-2}[\text{Å}^{-2}]. \tag{3}$$

This means that neutrons of a few Å wavelength possess an energy of a few meV, which corresponds to typical excitations in solids. This perfect match of microscopic length and energy scales with the wavelength and energy of the neutron is one of the many reasons why neutrons are such a well adapted tool for the investigation of microscopic processes.

3.2 s-wave scattering

For the neutrons we consider here the nuclei with dimensions of 10^{-4} Å are point-like. As a consequence the scattering from these structure-less objects must be purely isotropic. Mathematically speaking we are dealing with pure s-wave scattering. The strength of this scattering is parametrized by a scalar that we denote as the scattering length b of the nucleus.[2] It is not necessary to derive the scattering length via an analysis of the strong interaction between the neutron and the nucleus. For our purposes it is sufficient to know its experimentally determined value, which can be found tabulated.[3]
The scattering length b depends on the spin channel through which the scattering takes place. We denote the scattering length associated with the $2i+2$ states of spin $i+1/2$ as $b^{(+)}$ and that associated with the $2i$ states of spin $i-1/2$ as $b^{(-)}$.
Neutron scattering is in many respects not to different from light or X-ray scattering. It is, therefore, possible to apply principles familiar from classical optics. The main difference resides in the fact that the dispersion of a material wave differs from that of light because the Schrödinger equation is first order in time, whereas the Helmholtz equation is second order in time.
Light scattered from a point-like particle can be described as a superposition of spherical waves of the form

$$\psi(r, \theta, \phi) = A\frac{e^{i(\omega t - kr)}}{r}. \tag{4}$$

[2] b is a complex number. The imaginary part of b describes the absorption of neutrons by the nucleus.

[3] The scattering lengths are given for bound nuclei, that have no possibility to recoil in the course of the scattering. This fact has to be kept in mind when considering scattering from light atoms as e.g. hydrogen weakly adsorbed to surfaces.

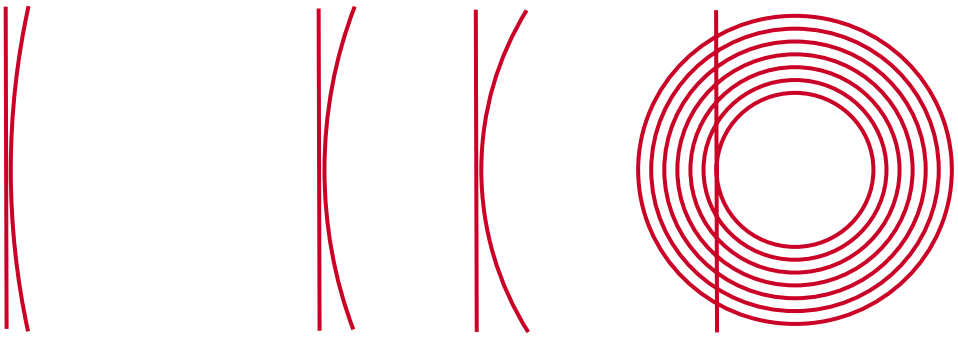

Figure 5: For large distances and sufficiently small volumes the spherical wave can be approximated by a plane wave.

For the observer the scattered light is indistinguishable from that of a point-like light source. Exactly the same holds for neutrons. The whole task of analyzing the data consists in correctly summing these spherical waves as they are scattered by the different constituents of our sample.

3.3 Double differential cross sections

Normally the distances between source and sample as well as between sample and detector are of the order of meters and thus much longer than the distances of a few Å investigated within the sample. For sufficiently large distances from the source and within sufficiently small space and time volumes a spherical wave can always be considered as plane (see figure 5). The interference phenomena arising from the scattering by an ensemble of scatterers can thus be treated in the classical way, i.e. by the transition probabilities involving only plain waves.
What we observe in the scattering experiment is the change in direction and energy of the incoming neutrons as sketched in figure 6.
The double differential scattering cross-section

$$\frac{d^2\sigma}{d\Omega dE'} \tag{5}$$

gives us *the number of neutrons scattered into a solid angle element* $d\Omega$ *with energies comprised between* E' *and* $E' + dE'$ *and normalized to the incoming flux.*

3.4 Born Approximation and master equation

If we assume that the incoming wave is not much perturbed by the scattering which is equivalent to saying that the scattered wave has a small amplitude even close to the scattering particle, then we can work in lowest order perturbation theory, i.e. in the so-called Born approximation. Due to the rather weak scattering amplitude of neutrons (the scattering length is very much smaller than the interparticle distances

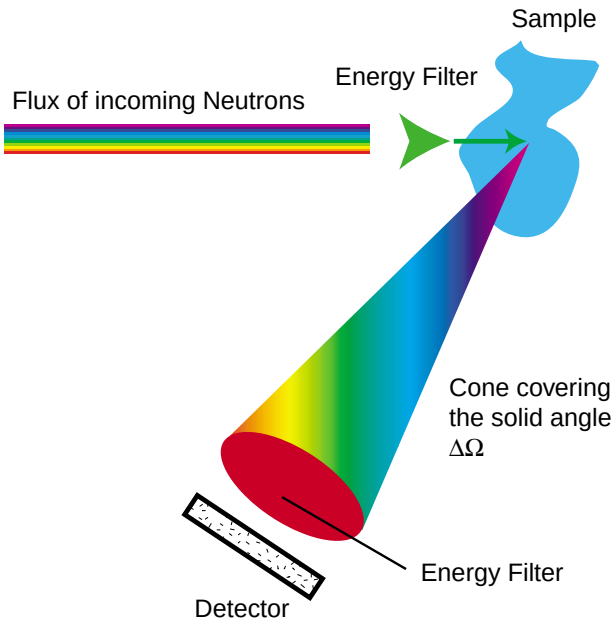

Figure 6: Schematics of a typical scattering experiment. In practice the change in energy and to some extent also the change in direction can be determined in various more or less sophisticated ways. The art of spectrometer design consists in making the observation of the double differential cross-sections as efficient as possible within the range of momentum and energy transfer of interest.

in the sample) this approximation holds in most practical cases.[4] The scattering from an ensemble of nuclei in the Born approximation is given by the sum of the scattering amplitudes (not the intensities) over the volume of coherence of the incoming and outgoing waves (see figures 7 and 8).
Using Fermi's Golden Rule we obtain for the crossection within the Born approximation

$$\frac{d^2\sigma}{d\Omega dE_f} = \frac{k_f}{k_i} \sum_{\lambda_i,\lambda_f} p_{\lambda_i} | < \vec{k}_f \sigma_f; \lambda_f | \mathbf{V} | \vec{k}_i \sigma_i; \lambda_i > |^2 \delta(\hbar\omega + E_{\lambda_i} - E_{\lambda_f}). \tag{6}$$

$\vec{k}_f$ and σ_f denote the wavevector and spin of the scattered neutron. Summation takes place over all accessible initial and final states of the sample. λ_i and λ_f stand for the ensemble of quantum numbers characterizing these states. The function p_{λ_i} weights the initial states according to the thermodynamic conditions and thus contains e.g. the temperature factor. The prefactor k_f/k_i originates in the normalization of the cross-

[4]The Born approximation fails for scattering which is highly concentrated in particular solid angles. A typical example for such scattering is Bragg scattering in highly pure crystals. In these cases we have to deal with the problem of extinction. Extinction can only be treated with dynamical scattering theory which allows for a coherent superposition of incoming and scattered wavefunctions [4]. It seems more or less excluded that extinction could be observed for inelastic signals even in highest purity silicon.

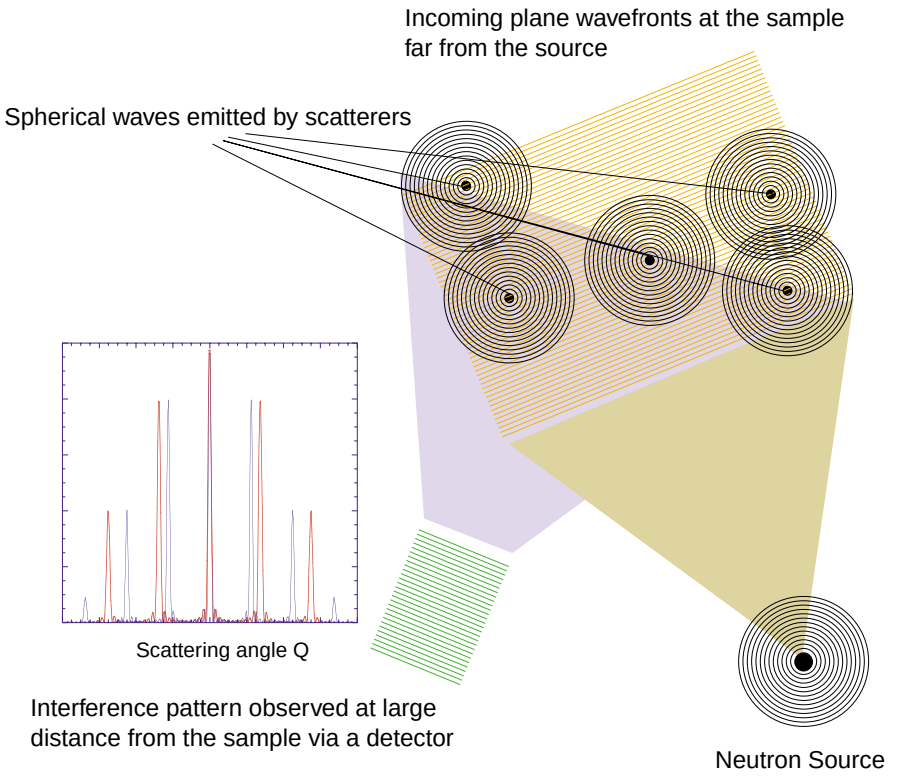

Figure 7: Theoretical principle underlying a scattering experiment. Spherical matter waves are emitted by the neutron source. For convenience we assume that they have a well-defined wave-length λ. At the sample, which is far from the source the waves emanating from individual source points have acquired planarity over sufficiently small distances. The scattering particles hit by the incoming waves send out spherical waves. If the particles have the same scattering length b then this is done coherently, i.e. there exists a well-defined phase relation among those waves leading to interference at the detector position.

section to the incident neutron flux and takes care of the density of scattered neutrons $\rho_{k_f}(E_f) = mk_f/\hbar^2$ within $d\Omega dE_f$.
The only potential leading to isotropic scattering in the Born approximation is the so-called Fermi pseudopotential

$$\mathbf{V}(\vec{r}) = \frac{2\pi\hbar^2}{m} \sum_l b_l \delta(\vec{r} - \vec{r}_l); \quad l = 1 \ldots N, \tag{7}$$

with $\vec{r}_l$ denoting the position of the nucleus l.[5] The prefactors are chosen such that the total scattering cross-section integrated over all angles for an isolated scatterer is given by

$$\sigma = 4\pi|b|^2. \tag{8}$$

[5]Please note that the δ-function has the dimensions of an inverse volume. So the scattering length b_l has the correct dimensions of a length.

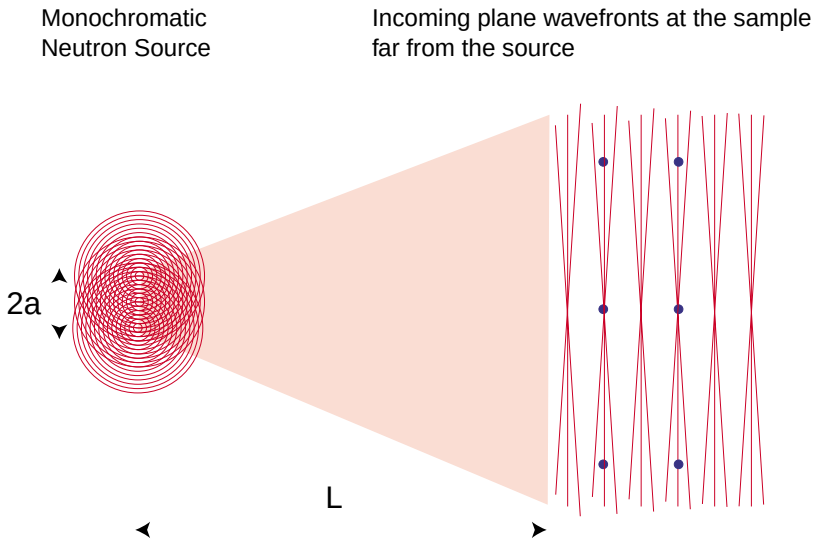

Figure 8: Coherence volumes. The wavefronts generated at the sample by different source points are tilted with respect to each other. The intesities of the interference patterns triggered by these wavefronts have to be added at the detector position. This leads to smearing of the signal. The amount of tilt that can still be tolerated defines the coherence volume [2]. The criterium for coherence is thus is somewhat arbitrary. The lateral coherence x_c of a monochromatic wave created by a source of width $2a$ is gives as $x_c = \frac{\lambda}{2\pi}\frac{L}{a}$. If we take $\lambda = 2\pi = 6.28\,\text{Å}$ then the lateral coherence length is $1000\,\text{Å}$. Only particle correlations at distances smaller that $1000\,\text{Å}$ would be observable in such an experiment.

Plugging eq. 7 into eq. 6 leads to the so-called master equation of neutron scattering

$$\frac{d^2\sigma}{d\Omega dE_f} = \frac{1}{N}\frac{k_f}{k_i}\sum_{\lambda_i,\sigma_i} p_{\lambda_i} p_{\sigma_i} \sum_{\lambda_f,\sigma_f} |<\sigma_f;\lambda_f|\sum_l b_l e^{i\vec{Q}\cdot\vec{r}_l}|\sigma_i;\lambda_i>|^2 \delta(\hbar\omega + E_{\lambda_i} - E_{\lambda_f}), \quad (9)$$

with $\vec{Q} = \vec{k}_i - \vec{k}_f$. We assume that neutrons are detected independent of their spin. This is why have to sum over σ_f. The δ-function indicates the conservation of energy. The energy lost or gained by the neutron is taken up or provided by the sample, respectively.

3.5 Typical neutron spectrometers

The basic scattering principle can in practice be realized in many different ways. As we have said before a well-performing spectrometer should deliver a high flux of neutrons with a sufficiently large coherence at the sample position. Like in optics the lack of coherence leads to the loss of interference. Without interference it is impossible to determine the space time arrangement of the scatterers. The same statement holds if we have good coherence but insufficient intensity to extract the correlation functions from the data. Neutron spectrometers can be classified according to the way they filter energies in order to prepare more or less monochromatic beams.

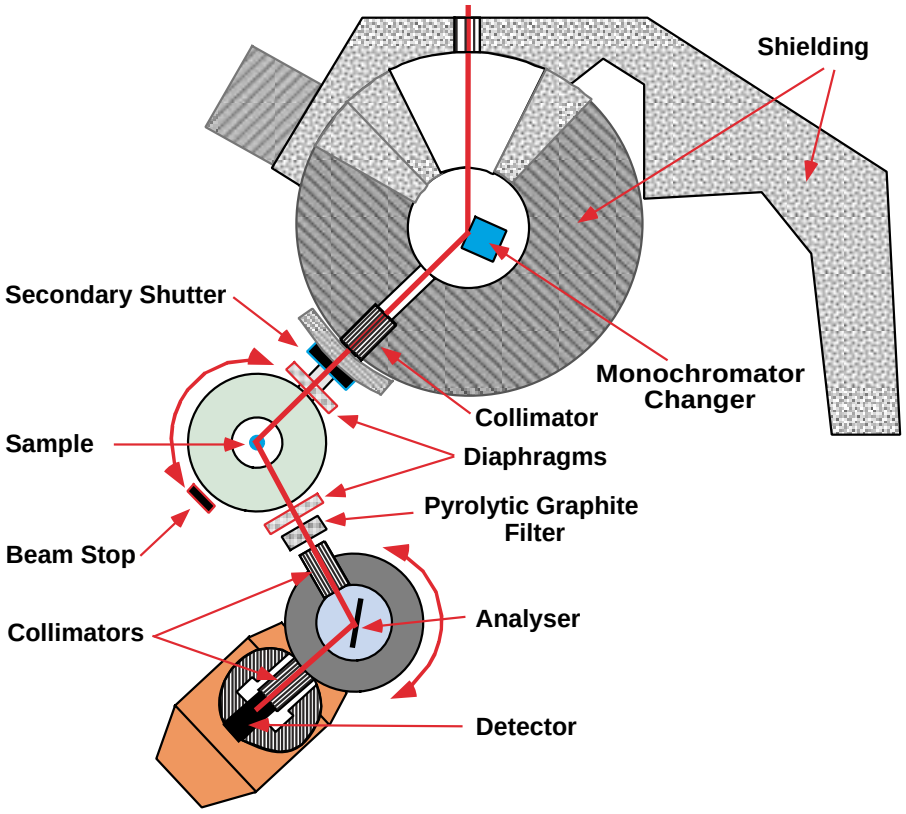

Figure 9: Schematic picture of a three axis instrument (courtesy of Arno Hiess, ILL). The white incoming neutron beam is monochromatized via Bragg reflection and scattered by the sample. The scattered beam is intercepted by an analyzer place at the scattering angle 2θ. The analyzer filters the neutrons according to their energy before they are detected. By changing monochromator, sample and analyzer angles it is possible to do point by point measurements along any trajectory in $(\vec{Q}, \omega)$-space accessible to the instrument.

3.5.1 Crystal spectrometers

In pure crystal spectrometers the filtering is done via Bragg-scattering. In the case of a three-axis machine monochromator and analyzer allow to fix both $\vec{k}_i$ and $\vec{k}_f$. The sample can be oriented in arbitrary positions with respect to the scattering plain. In this way it is possible to measure any point in $(\vec{Q}, \omega)$ space within the dynamical range accessible to the spectrometer (see figure 9). A crystal diffractometer differs from a three-axis spectrometer by the fact that the final energy is not analyzed. The secondary spectrometer in this case is replaced by position sensitive detectors covering more or less extended solid angles.

3.5.2 Time of flight spectrometers

The principle of a time-of-flight spectrometer relies on the fact that particles with varying speeds separate when travelling. Energies can thus be determined by measuring

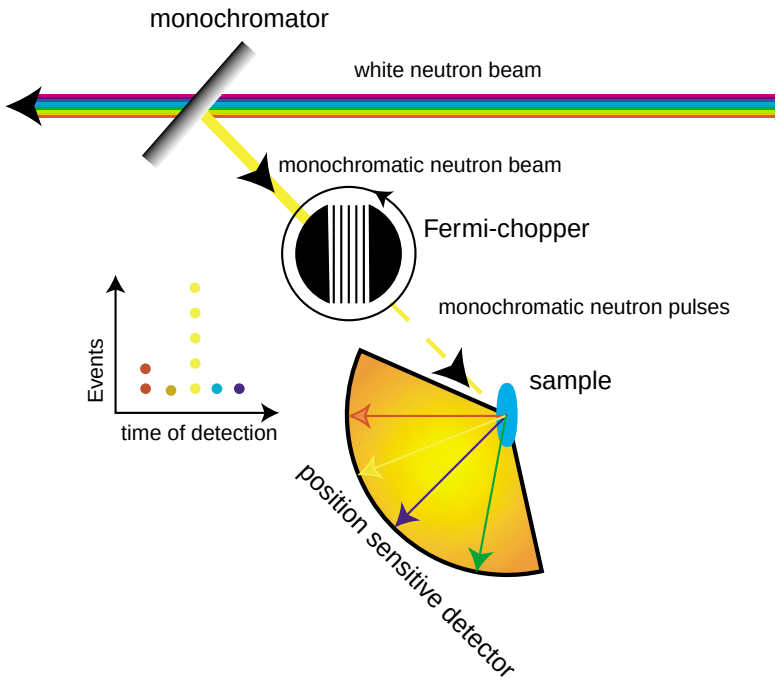

Figure 10: Schematic picture of a time-of-flight spectrometer. Monochromatization in this case is obtained via a crystal. The monochromatic beam is then chopped into pulses by a turning drum with a well-defined opening of a few degrees. The monochromatic neutron pulses are scattered by the sample into all directions. According to wether they have gained or lost energy they will arrive earlier or latter in the position sensitive detector. Thus both the change in energy and momentum can be measured over a wide range simultaneously. The prize to pay is the reduced intensity at the sample due to the pulsing process.

the time of flight along a known distance L. To do so we have to know the time of departure. As neutrons apart from their spin carry no labels they could be identified by this is only possible by imposing the same departure times to all of them, i.e. by working with pulsed beams. The pulsing is achieved by turning devices commonly called choppers. The degree of monochromaticity relies strongly on the opening times of these devices. It is certainly advantageous in terms of efficiency if the neutron source itself is pulsed. Apart from pure time-of-flight spectrometers mixtures of crystal and time-of-flight analysis are possible (see figure 10).

3.6 Scattering function

It is possible to write the double differential cross section in the form

$$\frac{d^2\sigma}{d\Omega dE_f} = \frac{k_f}{k_i} N \frac{\sigma_t}{4\pi} S(\vec{Q}, \omega), \tag{10}$$

with $\sigma_t \equiv 4\pi < \overline{b^2} >= 4\pi N^{-1} \sum_i \overline{b_i^2}$ denoting the mean total scattering cross-section and the bar over the scattering length b_i denoting spin and isotope averaging.[6]
Expressing the δ-function in the master equation eq. 9 as a time integral and working in the Heisenberg representation of quantum mechanics we obtain for the scattering function[7]

$$S(\vec{Q},\omega) = \frac{1}{2\pi\hbar N < \overline{b^2} >} \int_{-\infty}^{\infty} dt e^{-i\omega t} \sum_{k,l}^{N} \overline{b_k b_l} < e^{-i\vec{Q}\cdot\vec{r}_k} e^{i\vec{Q}\cdot\vec{r}_l(t)} > . \qquad (11)$$

$S(\vec{Q},\omega)$ is equally called dynamic structure factor.[8]
The scattering function $S(\vec{Q},\omega)$ has the dimension of an inverse energy and does not contain variables referring to the wavefunctions of the incoming and scattered neutrons. The relevant parameters are the momentum transfer $\vec{Q} = \vec{k}_i - \vec{k}_f$ and energy transfer $\hbar\omega = E_i - E_f$. How these transfers are realized in the experiment is from the purely theoretical point of view irrelevant for the physical result.[9] Eq. 10, therefore, states the fact that we can decoupled the probe from the system investigated. This is another important feature of neutron scattering that has its origin in the fact that the neutrons, because they are a very weak probe, monitor the unperturbed sample state. In other words, the experiment yields direct information on the spontaneous fluctuations in the sample, and this despite the fact that the neutrons interact with it.[10] This circumstance is mathematically expressed in the fluctuation dissipation theorem [1].

3.7 Coherent and incoherent scattering

If there is no exchange interaction between neighboring nuclei then the distribution of nuclear spins in the sample may be considered at all temperatures interesting to the solid state scientist as random. The same randomness is certainly found for the isotope distribution. In this case the double differential cross section separates into two parts.

[6] We will assume in the following that the scattering lengths are real, i.e. we omit absorption.

[7] We do not want to detail this procedure here, but refer the reader to the literature [1].

[8] As can be seen $S(\vec{Q},\omega)$ contains the scattering lengths b_l. The decoupling of probe, i.e. neutrons and sample is, therefore, incomplete. Only for a system featuring only a single scattering length $S(\vec{Q},\omega)$ becomes a quantity exclusively determined by the samples fluctuations. This is extremely convenient as in this case $S(\vec{Q},\omega)$ can be calculated via linear response theory without reference to the experiment. We will see later how the fact that the scattering lengths enter $S(\vec{Q},\omega)$ complicates the extraction of sample specific information e.g. in the case of inelastic neutron scattering data.

[9] This statement naturally does not hold for the real world. In an actual experiment neither the incoming nor the detected neutrons are exactly defined. The theoretical result, therefore has to be convoluted with the resolution function of the spectrometer, which is dependent explicitly on $\vec{k}_i$ and $\vec{k}_f$.

[10] The situation is analogous to probing a classical pendulum by driving it externally at small amplitudes. Only in a very small range of drive frequencies ω centered about the eigenfrequency ω_0 of the pendulum do we observe resonance. As the resonance frequency is independent of the driving force we probe via this experiment the intrinsic properties of the unperturbed system.

$$\frac{d^2\sigma}{d\Omega dE_f} = \left(\frac{d^2\sigma}{d\Omega dE_f}\right)_{\text{coherent}} + \left(\frac{d^2\sigma}{d\Omega dE_f}\right)_{\text{incoherent}} = \frac{k_f}{k_i}\frac{N}{4\pi}\left(\sigma_c S_c(\vec{Q},\omega) + \sigma_i S_i(\vec{Q},\omega)\right) \tag{12}$$

with

$$\sigma_c = 4\pi(\overline{b})^2 \tag{13}$$

$$\sigma_i = 4\pi\overline{(b^2)} - 4\pi(\overline{b})^2 \tag{14}$$

and

$$S(\vec{Q},\omega)_c = \frac{1}{2\pi\hbar N}\int_{-\infty}^{\infty} dt e^{-i\omega t}\sum_{k,l}^{N} < e^{-i\vec{Q}\cdot\vec{r}_k} e^{i\vec{Q}\cdot\vec{r}_l(t)} > \tag{15}$$

$$S(\vec{Q},\omega)_i = \frac{1}{2\pi\hbar N}\int_{-\infty}^{\infty} dt e^{-i\omega t}\sum_{l}^{N} < e^{-i\vec{Q}\cdot\vec{r}_k} e^{i\vec{Q}\cdot\vec{r}_l(t)} > \tag{16}$$

The first part is proportional to the square of the mean scattering length $(\bar{b})^2$. It is termed coherent and describes the interference arising from the coherent superposition of scattering amplitudes originating from all the scatterers.
The second part is proportional to the mean deviation of the scattering amplitude $(\overline{|b|^2} - |\bar{b}|^2)$. It is termed incoherent and contains only scattering terms $l = l'$ in eq. 9, i.e. those terms in the square of the sum involving the same particle.
The difference between coherent and incoherent scattering becomes most evident when we consider elastic scattering from a crystal. The coherent scattering as a function of scattering angle leads to Bragg-peaks containing information about the relative position of the atoms (see-figure 11). The incoherent scattering is absolutely flat and the only information we can extract from it is the number of scatterers.
The situation changes drastically when we consider atoms that move. In that case the wavefronts emitted at different times from the same particle are fully coherent leading to interference. The incoherent data then give valuable information on the single particle motions.

3.8 Self and distinct part of the scattering

Instead of the above chosen separation we may equally write

$$\frac{d^2\sigma}{d\Omega dE_f} = \frac{k_f}{k_i} N\left((\overline{b})^2 S_s(\vec{Q},\omega) + \overline{(b)^2} S_d(\vec{Q},\omega)\right) \tag{17}$$

with

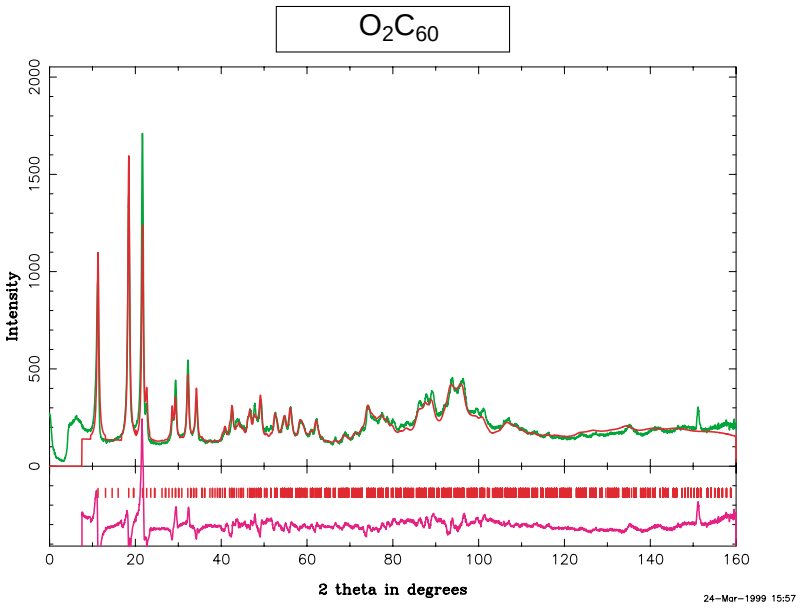

Figure 11: Diffraction pattern obtained on D2B of the ILL for a C_{60} sample containing oxygen. As both carbon and oxygen are completely coherent scatterers the amplitudes of the scattered waves have to be superimposed, leading to clear interference effects as a function of scattering angle. From the observed pattern it is possible to extract the orientation of the buckyballs and the positions of the oxygen atoms. If we had taken a spectrum from solid crystalline hydrogen it would be completely flat. The spin incoherent scattering would dominate completely. Despite the fact that we would be dealing with an ordered crystal it would be impossible to derive the order from the neutron data.

$$S(\vec{Q},\omega)_s = \frac{1}{2\pi\hbar N}\int_{-\infty}^{\infty} dt e^{-i\omega t} \sum_{k,l,l\neq k}^{N} < e^{-i\vec{Q}\cdot\vec{r}_k} e^{i\vec{Q}\cdot\vec{r}_l(t)} > \tag{18}$$

$$S(\vec{Q},\omega)_d = \frac{1}{2\pi\hbar N}\int_{-\infty}^{\infty} dt e^{-i\omega t} \sum_{l}^{N} < e^{-i\vec{Q}\cdot\vec{r}_k} e^{i\vec{Q}\cdot\vec{r}_l(t)} > \tag{19}$$

The first expression relates to the scattering arising from the interference of waves emanating from distinct particles only. The second expression describes the scattering from one and the same particle in the course of time. As can be seen the incoherent scattering is strictly of the same form as the self-scattering while in the coherent scattering we find contributions both from the self and distinct part.

3.9 Generalized susceptibility

Very often experimental results are presented in terms of the generalized susceptibility defined via

$$S(\vec{Q},\omega) = \frac{1}{\pi}\{1+n(\omega)\}\chi''[\omega]. \tag{20}$$

with the thermal occupation factor

$$n(\omega) = \frac{1}{e^{\frac{\hbar\omega}{k_b T}} - 1}. \tag{21}$$

Due to the dissipation fluctuation theorem the function $\chi''[\omega]$ has to be identified with the generalized susceptibility of the system, i.e. with the linear response of the system to a periodic perturbation of frequency ω. In the case of nuclear scattering the perturbation is a density fluctuation.[11] Generalized susceptibility means that the response refers to a perturbation that couples to the system via the scattering length of the neutron. For a one-component system it is identical to the real susceptibility.
A particularly instructive case is the scattering by harmonic lattice vibrations. For a simple harmonic oscillator the susceptibility is

$$\begin{aligned} \chi''[\omega] &= \frac{\pi}{2m\omega_0} \{\delta(\omega - \omega_0) - \delta(\omega + \omega_0)\} \\ &= \frac{1}{2m\omega_0} \{[1 + n(\omega_0)]\delta(\omega - \omega_0) + n(\omega_0)\delta(\omega + \omega_0)\} \end{aligned} \tag{22}$$

$\chi''[\omega]$ for a set of uncoupled harmonic oscillators is, therefore, independent of temperature (see figure 12).

3.10 Correlation functions

The particle density of a monatomic sample is given as

$$\hat{\rho}(\vec{r}, t) = \sum_j \delta\left(\vec{r} - \vec{R}_j(t)\right). \tag{23}$$

$\vec{R}_j(t)$ denotes the position of nucleus j at time t. It can be shown that the scattering function in that case may be expressed as the space and time Fourier transform of the density-density correlation function,i.e,

$$S(\vec{Q}, \omega) = \frac{1}{2\pi\hbar} \int_{-\infty}^{\infty} dt e^{-i\omega t} \int d^3 r e^{i\vec{Q}\cdot\vec{r}} G(\vec{r}, t) \tag{24}$$

with

$$G(\vec{r}, t) = \frac{1}{N} \int d^3\vec{r}' < \hat{\rho}(\vec{r}' - \vec{r})\hat{\rho}(\vec{r}', t) > . \tag{25}$$

The scattering experiment thus gives us information about the probability of finding a nucleus j at time t if there was a nucleus j' at time t'. This is not surprising given the fact that we observe the interference of spherical waves emanating from point-sources at positions $\vec{r}, \vec{r}'$ and times t, t'. The fact that we are dealing with an observation in

[11] For magnetic scattering the susceptibility relates to the response of the system perturbed by a magnetic field. We thus see that the neutrons in that case probe directly the electronic system.

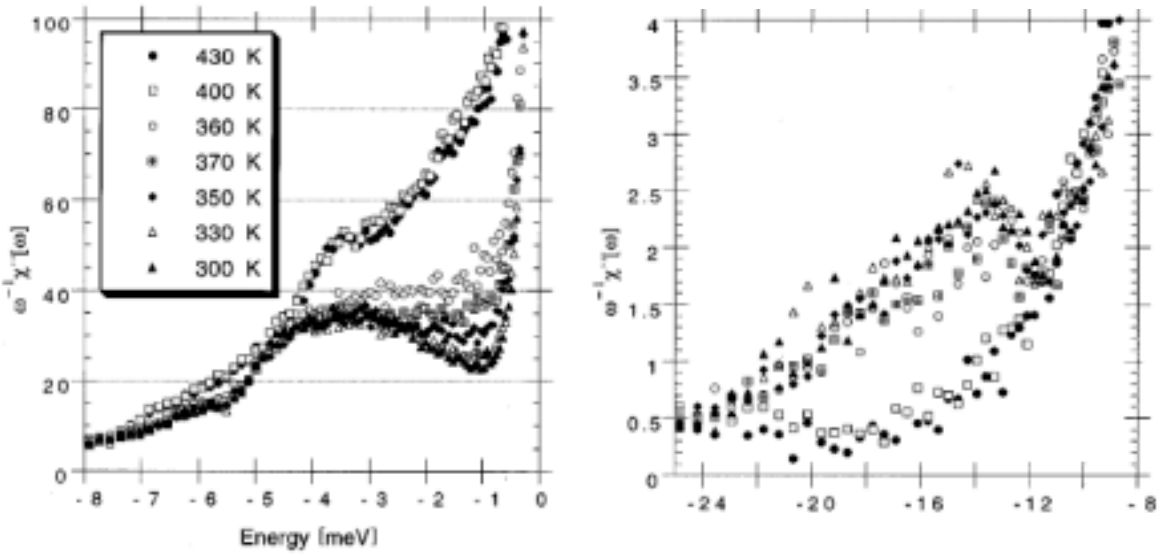

Figure 12: The generalized susceptibility for a sample of RbC_{60} as measured at the instrument IN6 of the ILL. Scattering from different angles has been summed. It can be seen that the system behaves harmonic between 300 and 350 K. Above that temperature the susceptibility increases at low energies (left) and disappears at high energies (right). The reason for this is a change in the state of the sample. The increase arises from rotational motion of the buckyballs. This motion is possible because they are no longer bound in polymeric chains. The break-up of the chains creates the loss of intensity at higher energies as the system no longer sustains the polymeric chain modes. The susceptibility is divided by ω to make it resemble as closely as possible the dynamic structure factor.

reciprocal space, i.e. a time and space Fourier transform is a direct consequence of the observation of this interference at large distances.
In many cases it is interesting to consider only the time Fourier transform of the scattering function, which is equivalent to the space Fourier transform of $G(\vec{r}, t)$

$$I(\vec{Q}, t) = \int e^{i\omega t} S(\vec{Q}, \omega). \tag{26}$$

An example is shown in figure 13.
By identifying the scattering function with the time-space Fourier transform of the particle density correlator we can make two interesting statements:

1. The limit $t \to 0$, i.e. the instantaneous correlation of particle positions is reached by integrating the observed scattering over all energies. This is typically done in a diffraction experiment. Diffraction thus does not measure the elastic scattering. It gives a snap shot of the sample.

2. If we measure purely elastic scattering then this corresponds to probing correlation at infinite times. In crystals the positions of the atoms are correlated over

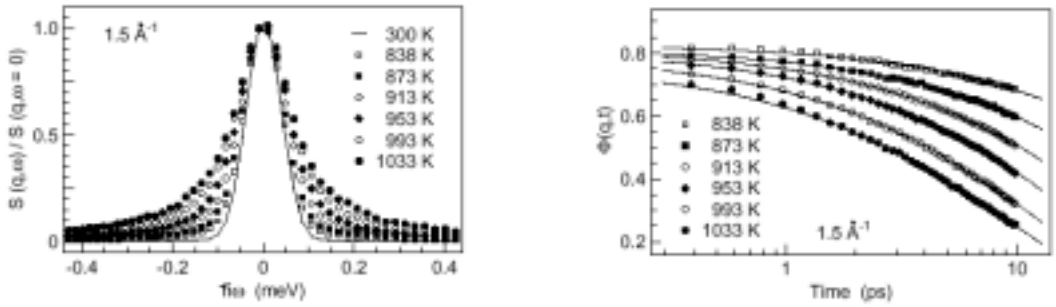

Figure 13: Scattering law (left panel) $S(\vec{Q},\omega)$ as measured for a complex metallic glass former for $\vec{Q} = 1.6\,\text{Å}^{-1}$ as a function of temperature. Fourier transformation in time leads to the intermediate scattering function shown on the right. The inelastic intensities observed in the experiment have their origin in relaxation processes. They lead to the decay of particle-particle correlations on microscopic time scales as directly seen in the intermediate scattering function. As the sample is cooled these relaxations slow down and finally freeze out below T_c.[5]

infinitely long times. The elastic scattering corresponds to the Bragg peaks. In liquids particles move in a random way. Correlations thus die out more or less quickly. Liquids thus have no elastic scattering.

References

[1] S.W. Lovesey, *Theory of Neutron Scattering from Condensed Matter*, Oxford University Press, Oxford (1984)

[2] J. Felber, R. Gähler, R. Golub, and K. Prechtl, *Coherence volumes and neutron scattering*, Physica B **252**, 34 (1998)

[3] C. Cohen-Tannoudji, B. Diu, and F. Laloë, *Méchanique Quantique*, Tome I et Tome II Hermann Éditeurs des Sciences et des Arts, Paris (1977,1986)

[4] V.F. Sears, *Neutron Optics*, Oxford University Press, New York (1989)

[5] A. Meyer, R. Busch, and H. Schober, *Time-Temperature Superposition of Structural Relaxation in a Viscous Metallic Liquid*, Phys. Rev. Lett. **83**, 5027-5029 (1999)